

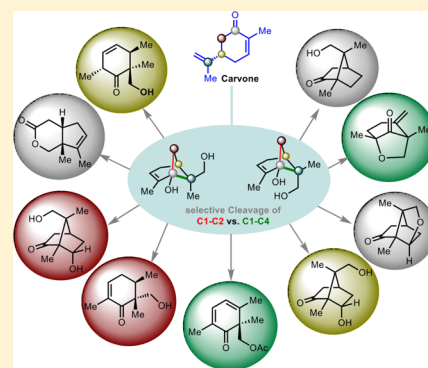
Selective C–C and C–H Bond Activation/Cleavage of Pinene Derivatives: Synthesis of Enantiopure Cyclohexenone Scaffolds and Mechanistic Insights

Ahmad Masarwa, Manuel Weber, and Richmond Sarpong*

Department of Chemistry, University of California, Berkeley, California 94720, United States

S Supporting Information

ABSTRACT: The continued development of transition-metal-mediated C–C bond activation/cleavage methods would provide even more opportunities to implement novel synthetic strategies. We have explored the Rh(I)-catalyzed C–C activation of cyclobutanols resident in hydroxylated derivatives of pinene, which proceed in a complementary manner to the C–C bond cleavage that we have observed with many traditional electrophilic reagents. Mechanistic and computational studies have provided insight into the role of C–H bond activation in the stereochemical outcome of the Rh-catalyzed C–C bond activation process. Using this new approach, functionalized cyclohexenones that form the cores of natural products, including the spiroindicumides and phomactin A, have been accessed.



INTRODUCTION

Carbon–hydrogen (C–H) and carbon–carbon (C–C) bonds are ubiquitous in organic molecules. As such, advances that accomplish the selective activation and functionalization of C–H and C–C bonds have the potential to revolutionize the synthesis of complex organic molecules. While methods for C–H activation/functionalization¹ have grown exponentially over the past decade, comparatively few methods for C–C bond activation have emerged.² General and effective methods for C–C activation are likely to change the practice of complex molecular synthesis just as C–H activation/functionalization logic is beginning to influence the synthesis of complex molecules.³ In particular, methods to selectively activate a desired C(sp³)–C(sp³) bond using transition-metal complexes remains difficult to achieve.² In order to make C–C bond activation processes broadly applicable in complex molecule synthesis, their scope and limitations need to be identified. This can be effectively achieved by exploring these methods in functional group rich, complex settings such as those encountered in natural product scaffolds. In this Article, we report our studies in this direction, which have focused on C–C bond activation/cleavage reactions of cyclobutanols, accessed in two steps from carvone, to yield functionalized cyclohexenone derivatives (e.g., **2** and **3**, Figure 1) that comprise the cores of several natural products. We also provide mechanistic insights into these Rh(I)-catalyzed transformations.

As a part of a general program to synthesize natural products including suaveolindol (**4**, Figure 1), phomactin A (**5**), spiroindicumides A and B (**6** and **7**), and others (**8–11**), we recognized that the core scaffold of these compounds could arise from sustainable, readily available, and inexpensive carvone.

A key challenge in achieving a unified strategy to these compounds (in particular **4–7**) would rely on identifying a divergent reaction on each enantiomer of carvone that would lead to the programmed installation of the C4 all-carbon quaternary stereocenter present in **2**, *ent*-**2**, **3**, and *ent*-**3** (see box in Figure 1).

RESULTS AND DISCUSSION

We commenced our studies with the conversion of (+)-carvone (**1**) to a diastereomeric mixture of epoxides (**12**; 1:1 d.r.) upon treatment with *m*-CPBA. Subjecting the diastereomers of **12** to *in situ* generated bis(cyclopentadienyl) titanium chloride (Cp₂TiCl) yields readily separable cyclobutanol-containing bicycles **13a** and **13b** (ratio of 3:2), following the precedent of Bermejo and co-workers.⁴ We have obtained unambiguous support for the structures of **13a** and **13b** using X-ray crystallographic analysis (see CYLviews in Scheme 1).⁵ This is a readily scalable route, and multigram quantities of **13a/b** can be accessed in a single pass.

We envisioned that diastereomers of **13** would serve as substrates in C–C bond activation and cleavage processes to yield substituted cyclohexenones such as **2** and **3** as well as the cores of **8–11**. As illustrated in Figure 2, complementary fragmentation scenarios could be imagined (e.g., for **13a**). While opening of the cyclobutane ring was anticipated on the basis of strain release considerations,⁶ it was unclear which proximal C–C bond would be cleaved (C1–C2 vs C1–C4). It was our expectation that through the appropriate choice of activating agent (transition-metal complex or traditional electrophiles/oxidants),

Received: March 4, 2015

Published: April 19, 2015

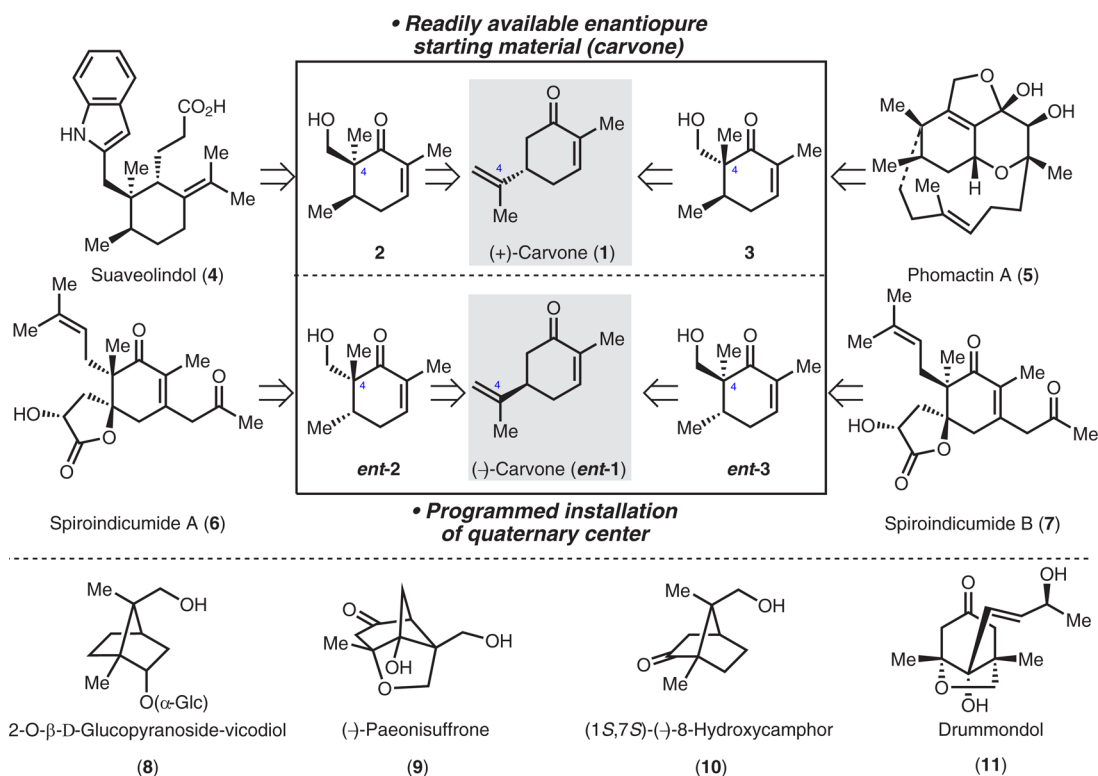


Figure 1. Unified, carvone-based strategy to natural product core scaffolds.

Scheme 1. Synthesis of Cyclobutanol Diastereomers 13a and 13b

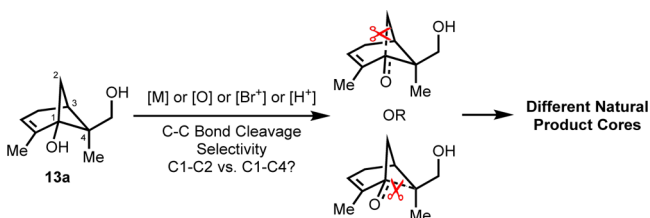
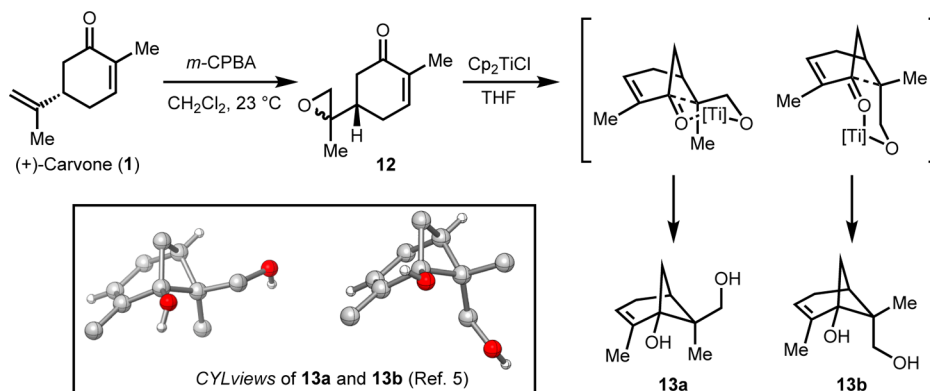


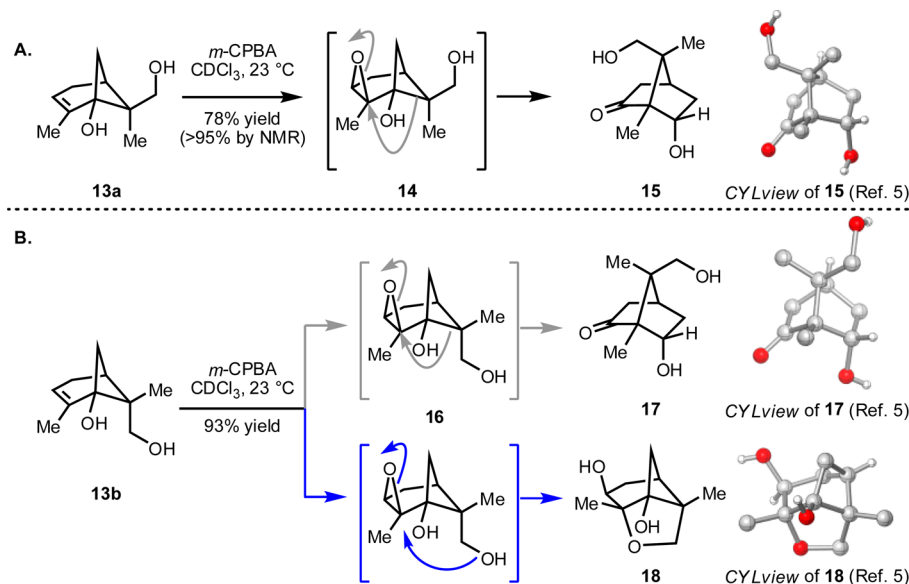
Figure 2. Proposed tactics for selective C–C bond cleavage in pinene derivatives, exemplified for 13a.

selectivity for the cleavage of either C–C bond could be achieved.

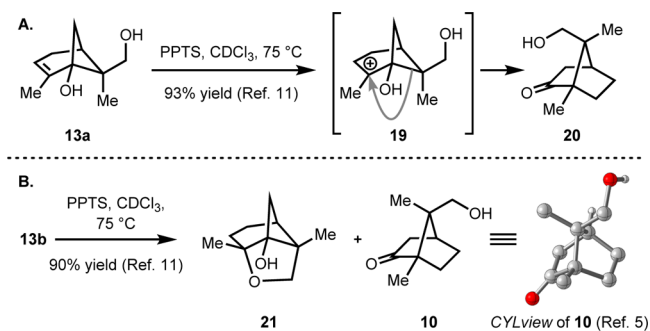
Despite the existing wealth of information on the skeletal rearrangements/fragmentations of pinene and associated derivatives,⁷ the rearrangement chemistry of hydroxylated variants such as 13a and 13b has not been investigated. Thus, we initiated our studies on the C–C bond activation/cleavage of 13a/b

using well-established reagents for the fragmentation/rearrangement of pinene (e.g., *m*-CPBA). Treatment of 13a with *m*-CPBA (Scheme 2A) leads to a diastereoselective epoxidation of the pinene derivative, which is then transformed to 15 (confirmed by X-ray crystallographic analysis) in 78% yield via 14. Similarly, 13b (Scheme 2B) rearranges to 17 and 18 (both confirmed by X-ray analysis) upon treatment with *m*-CPBA in 93% combined yield. Compound 17 (which maps on to the core of the natural product 8)⁸ arises from migration of the most substituted proximal C1–C4 bond (gray arrow in 16), whereas bridging tricyclic 18 (the core of the natural product 9)⁹ results from opening of the epoxide intermediate (blue arrow in 16) by the pendant primary hydroxy group.

In addition, when 13a was subjected to a Brønsted acid (PPTS) (Scheme 3A), the intermediate tertiary carbocation (19) rearranges to 20 as a result of the cleavage/migration of the more substituted C1–C4 bond. In the same fashion, 13b was transformed to naturally occurring 10¹⁰ and 21 (Scheme 3B),

Scheme 2. *m*-CPBA-Promoted Selective C1–C4 Bond Cleavage/Rearrangement of 13a and 13b^a

^a(B) When CDCl₃ was used as the reaction solvent, a 1:9 ratio of 17:18 was observed, whereas in CH₂Cl₂ a 1:3 mixture was formed.

Scheme 3. Products Formed During the PPTS-Initiated C–C Bond Cleavage/Rearrangement of 13a and 13b^a

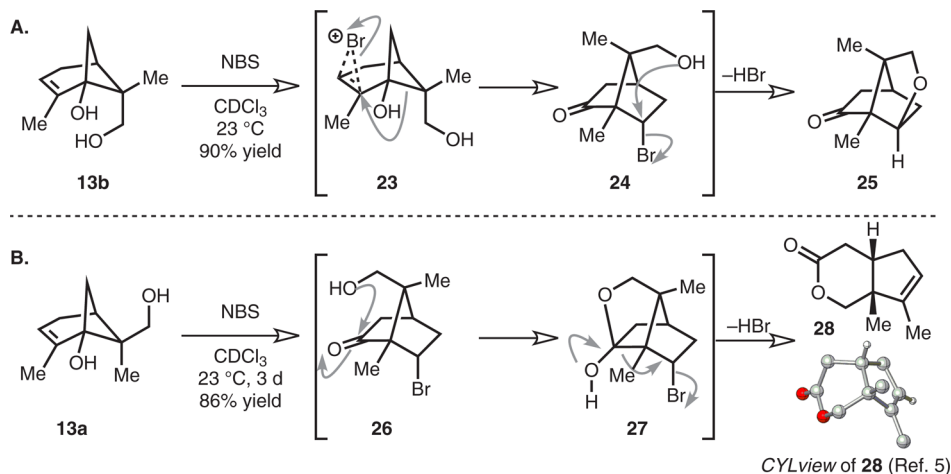
^aProducts 21 and 10 were formed in a 1:0.2 ratio alongside with a C1–C2 cleavage/rearrangement product.¹¹

where the incipient carbocation is intramolecularly intercepted by the primary hydroxy group.¹¹

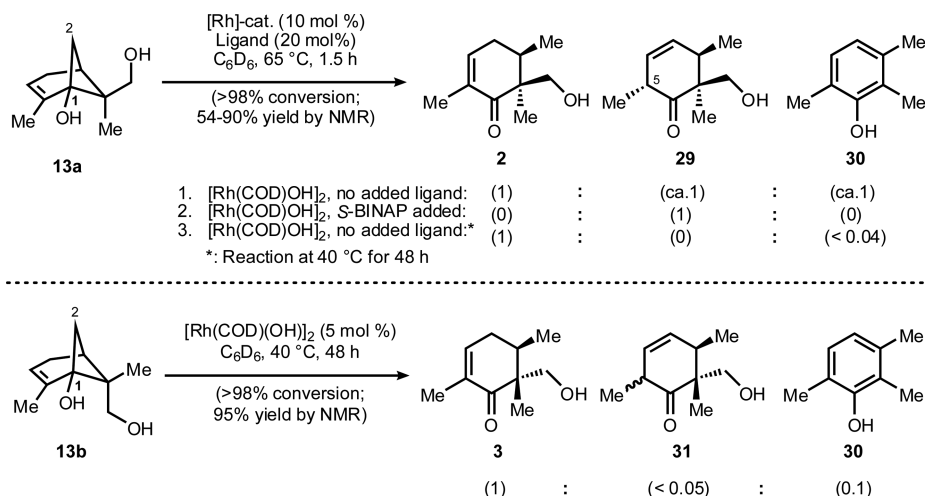
Treatment of 13b with *N*-bromosuccinimide (NBS) yields 25 (Scheme 4A), where a bridging ether linkage has formed via the intermediacy of 23 and 24, whereas exposure of diastereomer 13a to the same conditions gives lactone 28 via 26 and 27 (Scheme 4B).¹²

All the rearrangements of the pinene derivatives described thus far have involved the cleavage of the more substituted C1–C4 bond. In molecules such as 13, the C1–C4 bond is the weaker, longer bond (compare X-ray bond length in 13a: C1–C2 = 1.551 Å, C1–C4 = 1.567 Å; 13b: C1–C2 = 1.535 Å, C1–C4 = 1.589 Å). In addition, the cleavage of the C1–C4 bond favors the antiperiplanar relationship with either the epoxide (in 14 and 16; Scheme 2A,B) or the bromonium moiety (in 23; Scheme 4A,B). These observations are consistent with previous observations for pinene derivatives.^{7c} In order to access natural product cores such as 2 and 3, the less substituted, proximal C1–C2 bond has to be cleaved. To achieve this goal, we sought to employ transition-metal complexes. It is well established that transition-metal complexes can be sterically and electronically tuned (by the choice of metal or ligand) to exhibit a preference

Scheme 4. NBS-Promoted Selective C1–C4 Bond Cleavage/Rearrangement of 13



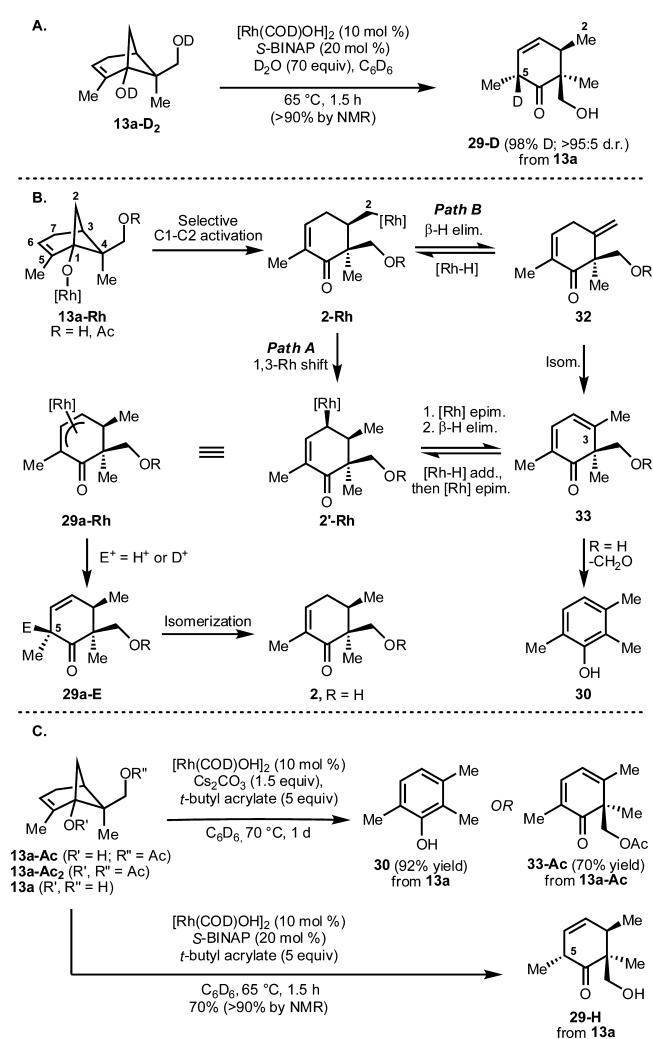
Scheme 5. Selective Rh-Catalyzed C1–C2 Bond Cleavage/Activation of 13



for the carbon (primary, secondary, or tertiary) on which the metal would reside on an incipient organometallic intermediate (e.g., primary C(sp³)-[M] species vs a tertiary C(sp³)-[M]). This outcome can either be thermodynamic (if the process is reversible) or kinetic (i.e., reflected in the transition-state energies).^{2,13} Over the past decade, significant advances have been made in the use of transition-metal complexes to facilitate the opening of strained cyclic compounds.¹³ Of the complexes that have been reported to effect these transformations, Rh-complexes have emerged as the most generally applicable.¹⁴

We initiated our Rh-catalyzed ring opening investigations using conditions developed by Murakami¹⁵ and by Cramer¹⁶ with 13a/b as the substrates (Scheme 5). Cyclohexenones 2 and 3 as well as 29 and 31 and phenol side product 30 were obtained following complete consumption of the starting material under the stated conditions. All of the observed products result from selective C1–C2 bond cleavage (C1–C4 ring opening products have not been observed). Following optimization, conditions to selectively access 2, 29, 3, as well as 30¹⁷ were identified.¹⁸ For diastereomer 13a, the addition of S-BINAP as a ligand to the standard conditions was beneficial¹⁹ and resulted in the formation of 29 as the exclusive diastereomer²⁰ (with respect to the C5 stereocenter, Scheme 5) in 70% isolated yield (90% by NMR). The formation of 2 as the major product could be achieved only when [Rh(COD)(OH)₂] was used as the catalyst at low temperature (see entry 3).²¹ At the lower temperature (i.e., 40 °C) phenol 30 was only observed in trace amounts, since the retro-aldol step that is required for its formation (see below) may require a higher temperature to proceed. A longer reaction time (Scheme 5, entry 3: 48 h vs entry 1: 1.5 h) allowed us to isomerize 29 to the thermodynamically favored conjugated enone 2 (compare also Scheme 5 bottom: isomerization of 31 to 3). However, with diastereomer 13b as the substrate, the standard conditions with a catalytic amount of [Rh(COD)(OH)₂] in the absence of S-BINAP proved superior, giving 3 in high yield.²²

Mechanistically, products 2 and 3 could arise from a simple protonolysis of the alkyl-Rh intermediate 2-Rh (Scheme 6B). However, a rationale for the formation of 29, 31, and 30 required further insight into the mechanism of the C–C bond cleavage process. To this end, exposure of 13a-Ac (Scheme 6C), bearing an acetyl group on the primary hydroxyl, to the reaction conditions led to clean conversion, suggesting that deprotona-

Scheme 6^a

^a(A) Deuteration studies; (B) mechanistic hypothesis of the Rh(I)-mediated transformations; (C) reactions with *t*-butyl acrylate as an additive. (add. = addition, elim. = elimination, epim. = epimerization).

tion of the primary hydroxyl in 13a is not a requirement for the Rh-catalyzed cyclobutanol opening. In contrast, bis-acetyl substrate 13a-Ac₂ did not react, which supports the importance of

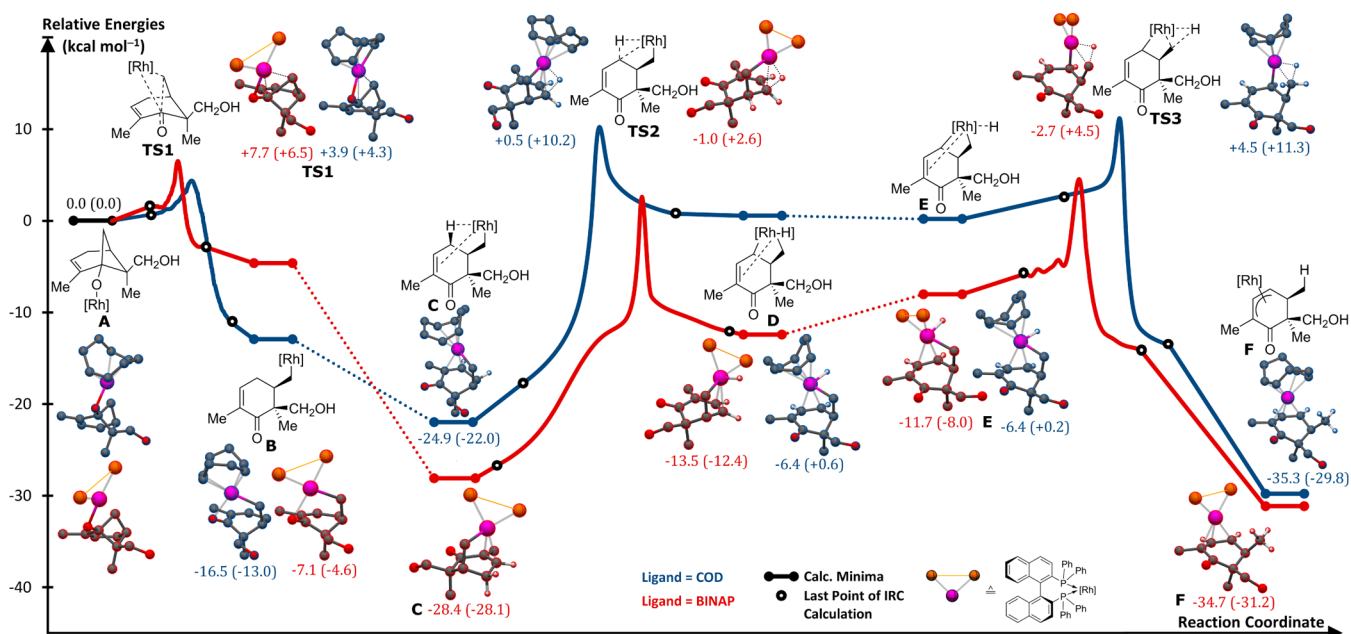


Figure 3. Energy profile of the C–C/C–H activation and reductive elimination steps for the transformation of 13a-Rh → 29a-Rh (A → F). Numbers represent relative energies reported in kcal mol⁻¹ at the DFT/M06-L/6-311+G(d,p)/LanL2DZ-F level in benzene and include zero-point energy correction. Numbers in brackets are gas-phase energies from IRC calculation and do not include zero-point energy correction.

deprotonation involving the tertiary hydroxy group of 13a to the cyclobutane opening step.²³ We have also conducted deuteration studies to gain more insight into the fate of the initially formed organo-Rh intermediate (i.e., 2-Rh). Using diastereomer 13a-D₂ (Scheme 6A) in the presence of D₂O, with [Rh(COD)OH]₂ as catalyst and S-BINAP as a ligand, we observed 98% D incorporation in 29-D at C5 and none at C2, indicating that the newly introduced hydrogen at C2 is likely delivered intramolecularly (but not from the primary hydroxy group). This newly introduced proton at C2 could either result from a 1,3-Rh shift²⁴ (Scheme 6B, Path A) or through a series of isomerization reactions (occurring by β-H elimination and readdition of [Rh–H]),²⁵ Scheme 6B, Path B). In Path A (i.e., after alkoxy-Rh 13a-Rh undergoes selective C1–C2 bond activation to give alkyl-Rh complex 2-Rh), an ensuing 1,3-Rh shift would yield π-allyl-Rh intermediate 29a-Rh via 2'-Rh. Metal enolate 29a-Rh may be protonated or deuterated to give 29a-E as a single diastereomer. This diastereoselectivity could arise from the fact that the primary OH/OD group triggers the protonation/deuteration, since a mixture of diastereomers (29a-E) is observed for the protonation of 29a-Rh, where R = Ac. However, this position (i.e., C5) is fairly acidic, and epimerization was observed when the reaction was allowed to proceed over longer periods and during silica gel chromatographic purification. However, in the crude reaction mixture, only a single diastereomer was observed, i.e., 29a-E (where E, R = H, D). Alternatively, in Path B, alkyl-Rh intermediate 2-Rh or the allylic Rh species (2'-Rh) may undergo β-H-elimination followed by isomerization to give 32/33, which converts to 30 by retro-aldol reaction.

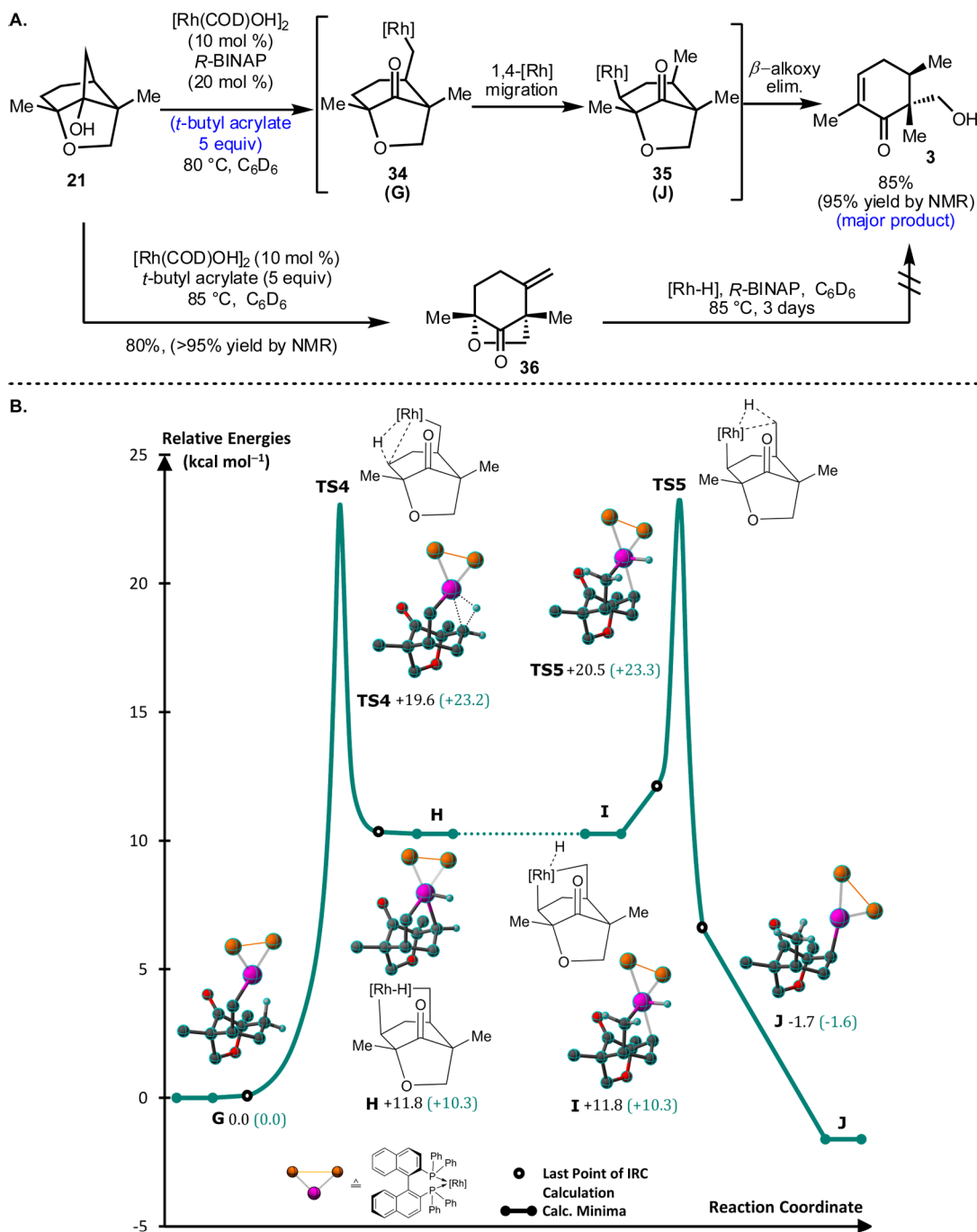
In an attempt to intercept the presumed [Rh–H] species that may be generated from 2-Rh, we added *t*-butyl acrylate as a [Rh–H]-acceptor (Scheme 6C). In the presence of *t*-butyl acrylate (5 equiv), 13a is converted to phenol 30 under the stated conditions. However, 13a-Ac, bearing an acetyl group, is selectively converted to 33-Ac under the same conditions, supporting the intermediacy of dienone 33²⁶ (where R = H, Scheme 6B) in the formation of phenol 30.²⁷ Changing the

ligand from COD to S-BINAP resulted in a substantial increase in the selectivity of the product formation (compare entries 1 to 2 in Scheme 5). An even more significant difference was observed when *t*-butyl acrylate was added to the reaction mixture; with COD as ligand, phenol 30 was obtained as the sole product (see Scheme 6C). On the other hand, using S-BINAP as the ligand (under otherwise identical conditions, Scheme 6C), 29-H was formed as the major product, without any trace of 30 observed. It therefore appears that when using S-BINAP as the ligand, a direct 1,3-Rh shift (Path A, Scheme 6B) is dominant over Path B. However, the mechanism of the 1,3-Rh migration¹⁶ remained to be fully elucidated.

On the basis of our combined observations, a 1,3-Rh migration would most likely occur through C–H activation involving 2-Rh.²⁸ In the expected C–H activation process, the Rh migrates from a thermodynamically less favored alkyl C(sp³) to a more favored allylic C(sp³) position, (see 2-Rh → 2'-Rh/29a-Rh, Scheme 6). The likelihood of such an allylic C(sp³)–H activation step is in agreement with the recent elegant observations of Lam and co-workers.²⁹ In their studies, the unexpected migration of Rh from a thermodynamically more favored vinyl C(sp²) to a less favored allylic C(sp³) position by C–H activation was observed.

To support the proposed C–H activation in the 1,3-Rh migration, we have undertaken computational analysis of the overall process (A → F) as summarized in Figure 3.³⁰

We found that the C–C bond activations (A → TS1 → B) with either COD (blue lines) or S-BINAP (red lines) as ligands show reasonable activation barriers of 3.9 and 7.7 kcal mol⁻¹, respectively. However, the most important difference was found in the stereospecific 1,3-Rh migration step by an oxidative C–H insertion and ensuing reductive elimination process (C → F via transition states TS2 and TS3). A total energy demand of 27.4 kcal mol⁻¹ was found when S-BINAP was modeled as the ligand and 29.4 kcal mol⁻¹ for COD. In general, these barriers indicate the feasibility of such a 1,3-Rh-migration through C–H activation. Although the barrier for the C–H activation (C → D) is lower when COD is modeled as the ligand (ΔΔG⁰ = 2.0 kcal⁻¹),

Scheme 7^a

^a(A) Selective Rh-catalyzed C–C/C–H activation for **21** and stereospecific synthesis of **36**. (B) Energy profile of the stereospecific 1,4-[Rh] shift **G** → **J** (**34** → **35**). Numbers represent relative energies reported in kcal mol⁻¹ at the DFT/M06-L/6-311+G(d,p)/LanL2DZ-F level in benzene and include zero-point energy correction. Numbers in brackets are gas-phase energies from IRC calculation and do not include zero-point energy correction.

the reductive elimination (**E** → **F**) was calculated to be lower by 3.7 kcal mol⁻¹ for the *S*-BINAP ligand. The lower overall barrier of the Rh-shift process for the *S*-BINAP system ($\Delta\Delta G^0 = 2.0$ kcal mol⁻¹) may indicate that with this ligand, a C–H activation scenario is kinetically more favored than in the case with COD as the ligand.

Experimentally, such a C(sp³)–H bond activation is supported by several observations. First, tricycle **21** (Scheme 7A) is converted to **3** upon exposure to a catalytic amount of the Rh-precatalyst and *R*-BINAP.

We believe this transformation proceeds via **34**, which following a net 1,4-Rh migration by C–H activation affords **35** that undergoes β -alkoxy elimination to give **3**. Of note, when **21** is subjected to the standard conditions (i.e., in the absence of *R*-BINAP, see Scheme 7A), the addition of *t*-butyl acrylate as a hydride acceptor leads to the exclusive formation of **36**,³¹ while in the presence of *R*-BINAP (blue highlighting in Scheme 7A), **3** is formed as the major product. These observations suggest that with BINAP as ligand, a stereospecific Rh-shift is dominant, whereas with COD as the ligand, β -H elimination becomes

significant, leading to a complex reaction mixture, presumably proceeding through an isomerization process.

For the transformation of **21** to **3**, the isomerization pathway²⁵ is very unlikely, since the readdition of [Rh–H], bearing the bulky *R*-BINAP ligand, would have to occur from the sterically less accessible α -face (i.e., concave face) of **36** in order to give **3** where both vicinal Me-groups are syn disposed.

The unlikelihood of a [Rh–H] isomerization pathway is further supported by the observation that in the reaction of cyclohexanone **36** with *in situ* generated [Rh–H], **3** is not observed as a product.³² The activation barrier for a stereospecific 1,4-Rh migration²⁸ proceeding by C(sp³)–H activation was computed at 19.6 kcal mol^{–1} (see Scheme 7B), and the barrier for the subsequent reductive elimination was computed as 8.7 kcal mol^{–1}, which are in agreement with reported systems.³⁰

CONCLUSION

In summary, a series of enantiopure cyclohexenone and cyclohexanone derivatives (e.g., **2**, **3**, **17**, and **36**) that comprise the cores of several natural products (**4**, **5**, **8**, and **11**, respectively) have been accessed from readily available carvone. Key to these transformations is a selective C–C bond activation/cleavage. Traditional electrophilic reagents as well as Rh(I) complexes were employed in order to achieve complementary C–C bond cleavages. Our mechanistic investigations into the Rh-catalyzed C–C activation indicate that a subsequent Rh migration most likely proceeds by C–H activation. To the best of our knowledge, this work represents the first observations of a stereospecific 1,3- and 1,4- C(sp³) to C(sp³) Rh-migration occurring through C–H bond activation. CCDC 1051272 (**10**), CCDC 1051273 (**13a**), CCDC 1051274 (**13b**), CCDC 1051275 (**15**), CCDC 1051276 (**17**), CCDC 1051277 (**18**), and CCDC 1051278 (**28**) contain the supplementary crystallographic data for this paper. These data can be obtained free of charge from The Cambridge Crystallographic Data Centre via www.ccdc.cam.ac.uk/data_request/cif.

ASSOCIATED CONTENT

Supporting Information

Experimental and computational details and analytical and supplemental data for the prepared compounds. This material is available free of charge via the Internet at <http://pubs.acs.org>.

AUTHOR INFORMATION

Corresponding Author

*rsarpong@berkeley.edu

Notes

The authors declare no competing financial interest.

ACKNOWLEDGMENTS

The authors thank the Rothschild Foundation and VATAT (The Israeli Council for Higher Education) for postdoctoral fellowships to A.M. and the DAAD (German Academic Exchange Service) for a postdoctoral fellowship to M.W. We thank Dr. A. DiPasquale for solving the crystal structures, supported by NIH Shared Instrument Grant (S10-RR027172) as well as NSF CHE-0840505 for funding computational resources at UCB and Dr. Kathleen Durkin for assistance with the computational studies. Funding was in part provided by the NSF under CCI center for selective C–H functionalization (CHE-1205646)

REFERENCES

- (1) For reviews see: (a) Ackermann, L. *Acc. Chem. Res.* **2014**, *46*, 281. (b) Engle, K. M.; Mei, T.-S.; Wasa, M.; Yu, J.-Q. *Acc. Chem. Res.* **2012**, *45*, 788. (c) Ackermann, L.; *Modern Arylation Methods*; Wiley-VCH: Weinheim, 2009. (d) Bergman, R. G. *Science* **1984**, *223*, 902.
- (2) (a) Murakami, M.; Ito, Y. in *Topics in Organometallic Chemistry*; Springer: Berlin, 1999; Vol. 3, pp 97. (b) Jun, C. H. *Chem. Soc. Rev.* **2004**, *33*, 610. (c) Rybtchinski, B.; Milstein, D. *Angew. Chem., Int. Ed.* **1999**, *38*, 870. (d) Marek, I.; Masarwa, A.; Delaye, P.-O.; Leibel, M. *Angew. Chem., Int. Ed.* **2015**, *54*, 414. (e) C–C Bond activation. *Topics in Current Chemistry*; Dong, G., Ed.; Springer: Berlin, 2014; Vol 346. (f) Ruhland, K. *Eur. J. Org. Chem.* **2012**, 2683. (g) Aissa, C. *Synthesis* **2011**, 3389. (h) Murakami, M.; Matsuda, T. *Chem. Commun.* **2011**, 47, 1100. (i) Park, Y. J.; Park, J.-W.; Junn, C.-H. *Acc. Chem. Res.* **2008**, *41*, 222. (j) Murakami, M.; Makino, M.; Ashida, S.; Matsuda, T. *Bull. Chem. Soc. Jpn.* **2006**, *79*, 1315. (k) Tunge, J. A.; Burger, E. C. *Eur. J. Org. Chem.* **2005**, 1715. (l) Jun, C.-H. *Chem. Soc. Rev.* **2004**, *33*, 610. (m) Perthuisot, C.; Edelbach, B. L.; Zubris, D. L.; Simhai, N.; Iverson, C. N.; Müller, C.; Satoh, T.; Jones, W. D. *J. Mol. Catal. A* **2002**, *189*, 157.
- (3) For a recent example, see: Yamaguchi, J.; Yamaguchi, A. D.; Itami, K. *Angew. Chem., Int. Ed.* **2012**, *51*, 8960.
- (4) Bermejo, F. A.; Mateos, A. F.; Escribano, A. M.; Lago, R. M.; Burón, L. M.; López, M. R.; González, R. R. *Tetrahedron* **2006**, *62*, 8933.
- (5) X-Ray structures were visualized with: Legault, C. Y. *CYLview*, 1.0b; Université de Sherbrooke: Quebec, Canada, 2009 (<http://www.cylview.org>). Most of the hydrogen atoms are removed for clarity.
- (6) Cyclobutanes have an inherent ringstrain of 28 kcal/mol, see ref 13a.
- (7) (a) Erman, M. B.; Kane, B. J. *Chem. Biodiversity* **2008**, *5*, 910. (b) Mann, J.; Davidson, R. S.; Hobbs, J. B.; Banthorpe, D. V.; Harborne, J. B. *Natural Products*; Addison Wesley Longman Ltd.: Harlow, UK, 1994; pp 309. (c) Bhattacharyya, P. K.; Prema, B. R.; Kulkarni, B. D.; Pradhan, S. K. *Nature* **1960**, *187*, 689.
- (8) Gan, L.-S.; Zhan, Z.-J.; Yang, S.-P.; Yu, J.-M. *J. Asian Nat. Prod. Res.* **2006**, *8*, 589.
- (9) (a) Shibata, S.; Nakahara, M. *Chem. Pharm. Bull.* **1963**, *11*, 372. (b) Aimi, N.; Inaba, M.; Watanabe, M.; Shibata, S. *Tetrahedron* **1969**, *25*, 1825. (c) Yoshikawa, M.; Harada, E.; Kawaguchi, A.; Yamahara, J.; Murakami, N.; Kitagawa, I. *Chem. Pharm. Bull.* **1993**, *41*, 630. (d) Martín-Rodríguez, M.; Galán-Fernández, R.; Marcos-Escribano, A.; Bermejo, F. A. *J. Org. Chem.* **2009**, *74*, 1798.
- (10) This is the first non-biotransformation based preparation of **10**; for an earlier preparation see: Miyazawa, M.; Miyamoto, Y. *J. Mol. Catal. B* **2004**, *27*, 83.
- (11) See the Supporting Information for additional details and rearrangements where a cleavage of the C1–C2 bond was observed.
- (12) Treating **13a** with Br₂ instead of NBS also forms lactone **28** in similar yield.
- (13) (a) Seiser, T.; Saget, T.; Tran, D. N.; Cramer, N. *Angew. Chem., Int. Ed.* **2011**, *50*, 7740. (b) Masarwa, A.; Marek, I. *Chem.—Eur. J.* **2010**, *16*, 9712.
- (14) (a) Murakami, M. *Chem. Rec.* **2010**, *10*, 326. (b) Cramer, N.; Seiser, T. *Synlett* **2011**, 449.
- (15) For a recent example, see: Yada, A.; Fujita, S.; Murakami, M. *J. Am. Chem. Soc.* **2014**, *136*, 7217.
- (16) Seiser, T.; Cramer, N. *J. Am. Chem. Soc.* **2010**, *132*, 5340.
- (17) See Scheme 6B for the selective synthesis of **30**.
- (18) The relative configurations of **2** and **3** were elucidated by NOESY experiments and ¹³C NMR calculations, see Supporting Information.
- (19) Using *R*-BINAP resulted in a “mismatch”, impeding the ring opening reaction and giving a complex reaction mixture.
- (20) The relative configuration of **29** was elucidated by NOESY NMR, see Supporting Information.
- (21) Product **2** can also be obtained by (a) treating **29** with a base (i.e., Cs₂CO₃, see Supporting Information) or (b) under the [Rh(COD)OH]₂ conditions and a longer reaction time.

- (22) For the most efficient access to **3**, see Scheme 7A.
- (23) The same results were obtained for diastereomers **13b-Ac** and **13b-Ac₂**.
- (24) For a 1,3-Rh shift by a proto-demetalation process see ref 16.
- (25) Matsuda, T.; Shigeno, M.; Murakami, M. *J. Am. Chem. Soc.* **2007**, *129*, 12086.
- (26) Importantly, dienone **33-Ac** could offer opportunities for oxygenation at C3 to access the spiroindicumides.
- (27) Diastereomers **13b** and **13b-Ac** gave similar results, see Supporting Information for details.
- (28) For examples of 1,4- and 1,5-Rh shifts from C(sp³) to C(sp²) by C–H activation, see: (a) Seiser, T.; Roth, O. A.; Cramer, N. *Angew. Chem., Int. Ed.* **2009**, *48*, 6320. (b) Ishida, N.; Shimamoto, Y.; Yano, T.; Murakami, M. *J. Am. Chem. Soc.* **2013**, *135*, 19103.
- (29) Burns, D. J.; Lam, H. W. *Angew. Chem., Int. Ed.* **2014**, *53*, 9931.
- (30) This setup was recently used in many DFT investigations for Rh-catalyzed reactions, see: Yu, H.; Wang, C.; Yang, Y.; Dang, Z.-M. *Chem.—Eur. J.* **2014**, *20*, 3839 and references therein. See the Supporting Information for further computational details.
- (31) For racemic access/isolation to such natural product (cores), see: (a) Nagaraju, C.; Prasad, K. R. *Angew. Chem., Int. Ed.* **2014**, *53*, 10997. (b) Shiao, H.-Y.; Hsieh, H.-P.; Liao, C.-C. *Org. Lett.* **2008**, *10*, 449. (c) Milborrow, B. V. *Phytochemistry* **1975**, *14*, 1045. (d) Powell, R. G.; Weisleder, D.; Smith, C. R. *J. Org. Chem.* **1986**, *51*, 1074.
- (32) Although we observe slow conversion of **36** (ca. 45% after 1 day, ca. 70% after 3 days), only unidentified side products were formed. See the Supporting Information for details.